

Controlled incorporation of deuterium into bacterial cellulose

Junhong He · Sai Venkatesh Pingali · Shishir P. S. Chundawat · Angela Pack ·
A. Daniel Jones · Paul Langan · Brian H. Davison · Volker Urban ·
Barbara Evans · Hugh O'Neill

Received: 20 June 2013 / Accepted: 18 September 2013 / Published online: 10 October 2013
© Springer Science+Business Media Dordrecht (outside the USA) 2013

Abstract Isotopic enrichment has been widely used for investigating the structural and dynamic properties of biomacromolecules to provide information that cannot be carried out with molecules composed of natural abundance isotopes. A media formulation for controlled incorporation of deuterium in bacterial cellulose synthesized by *Gluconacetobacter xylinus* subsp. *sucrofermentans* is reported. The purified cellulose was characterized using Fourier Transform Infra-Red spectrophotometry and mass spectrometry which revealed that the level of deuterium incorporation in the perdeuterated cellulose was greater than 90 %. Small-angle neutron scattering analysis demonstrated that the overall structure of the cellulose was unaffected by the substitution of deuterium for hydrogen. In addition, by varying the amount of *D*-glycerol in the media it was possible to vary the scattering length density of the deuterated cellulose. A

large disk model was used to fit the curves of bacterial cellulose grown using 0 and 100 % *D*-Glycerol yielding a lower bound to the disk radii, $R_{\min} = 1,132 \pm 6$ and $1,154 \pm 3$ Å and disk thickness, $T = 128 \pm 1$ and 83 ± 1 Å for the protiated and deuterated forms of the bacterial cellulose, respectively. This agrees well with the scanning electron microscopy analysis which revealed stacked sheets in the cellulose pellicles. Controlled incorporation of deuterium into cellulose will enable new types of experiments using techniques such as neutron scattering to reveal information about the structure and dynamics of cellulose and its interactions with proteins and other (bio) polymers.

Keywords Cellulose · Deuteration · Labeling · Small-angle neutron scattering · Mass spectrometry

J. He · S. V. Pingali · P. Langan · V. Urban ·
H. O'Neill (✉)
Biology and Soft Matter Division, Oak Ridge National
Laboratory, Oak Ridge, TN 37831, USA
e-mail: oneillhm@ornl.gov

S. P. S. Chundawat
Chemical Engineering and Materials Science, Michigan
State University, East Lansing, MI 48824, USA

A. Pack · B. Evans
Chemical Sciences Division, Oak Ridge National
Laboratory, Oak Ridge, TN 37831, USA

A. D. Jones
Department of Biochemistry and Molecular Biology,
Michigan State University, East Lansing, MI 48824, USA

A. D. Jones
Department of Chemistry, Michigan State University,
East Lansing, MI 48824, USA

B. H. Davison
Biosciences Division, Oak Ridge National Laboratory,
Oak Ridge, TN 37831, USA

Introduction

Cellulose, the most abundant of the carbohydrates, was originally isolated from its most familiar and widespread source, the cell walls of higher plants. Indeed, its name was derived based on its occurrence. Many algae, several fungi, certain bacteria, and a few marine animals such as tunicates also synthesize cellulose (Pérez et al. 2010). Chemically, cellulose is a biopolymer composed of linear, parallel chains of β 1-4-linked glucose units which are assembled into crystalline microfibrils during biosynthesis. Its crystalline, fibrous nature imparts special physical properties to cellulose that have made it an important material, particularly in the paper, pulp, and textile industries (Franz and Blaschek 1990). Expansion of cellulose utilization as an alternative, sustainable feedstock for production of fuels and materials is being investigated, with an emphasis on fuel ethanol production (Ragauskas et al. 2006). In plant cell walls, cellulose microfibrils are an integral part of the laminate structure, forming strong associations with lignin, hemicellulose, pectin, and proteins. Removal of the other cell wall components from cellulose in order to utilize it requires physical and chemical treatments that vary according to the intended use and which add to the expense of the process. Strategies to overcome this cell wall recalcitrance are being investigated (Himmel et al. 2007).

Bacterial cellulose is a type of pure cellulose that is synthesized by some species of acetic acid bacteria as an extracellular biofilm or membrane called a pellicle (Brown 1886; Schramm and Hestrin 1954; Cannon and Anderson 1991; Iguchi et al. 2000; Klemm et al. 2005). The bacteria known to synthesize cellulose exhibit typical characteristics of the genus *Acetobacter*: aerobic, gram-negative, do not require amino acid supplementation and can utilize ammonium as a nitrogen source, but require vitamin supplementation. They have been isolated from a wide range of environments, including vinegar, wine, kombucha, nata de coco, and spoiled fruit (Holt et al. 1994; Cannon and Anderson 1991; Iguchi et al. 2000). The amount of cellulose produced varies depending on the species and strain, with three species generally cited as producing the typical thick pellicle: *Acetobacter xylinus* (synonym *xylinum*), *hansenii*, and *pasteuriani* (Bernardo et al. 1998). The placement of these species in a separate genus *Gluconacetobacter* was proposed

(Yamada et al. 1997). As bacterial cellulose is not synthesized as a composite with other insoluble polymers but is extruded into the growth medium, it can be purified more easily than most plant-derived cellulose. Bacterial cellulose differs in its physical properties and higher structural organization from plant cellulose. In its natural state, it is a hydrogel containing 99 % water. As well as high water retention, it also possesses higher tensile strength and Young's modulus than purified plant cellulose (Iguchi et al. 2000). The physical properties of bacterial cellulose as well as the ease of purification have led to investigation of its potential as a material for a wide range of applications, including paper pulp, electronics manufacture, and fuel cells (Cannon and Anderson 1991; Iguchi et al. 2000; Shah and Brown 2005; Evans et al. 2003). Investigation of its potential use as a biomedical material for wound dressing and implants continues to expand (Czaja et al. 2007). Bacterial cellulose has been a useful model to elucidate the synthesis of cellulose. Investigation of cellulose synthesis by *Acetobacter xylinum* has established that the immediate precursor substrate used by the cellulose synthase complex is UDP-glucose, which is synthesized from glucose-1-phosphate and UTP (Cannon and Anderson 1991). Further investigation of the cellulose synthesis pathway established that several gene products were required to achieve high levels of production of crystalline cellulose (Saxena et al. 1994; Kawano et al. 2002).

However, the production of cellulose by *Acetobacter/Gluconacetobacter* species is complicated by their multiple metabolic pathways for utilization of carbohydrates, as well as by the variations between strains and the frequently observed instability of cellulose synthesis. Static growth conditions in shallow vessels with high surface area are known to favor cellulose pellicle formation (Brown 1886; Hestrin and Schramm 1954; Schramm and Hestrin 1954; Bernardo et al. 1998; Cannon and Anderson 1991). Agitation of the growth media resulted in inhibition of cellulose production, resulting in the formation of disorganized cellulose fragments. The non-cellulose producing (cel-) condition is observed as formation of smooth instead of rough colonies on agar plates (Schramm and Hestrin 1954; Bernardo et al. 1998; Cannon and Anderson 1991; Krystynowicz et al. 2002). Increase in medium viscosity by addition of agar was also observed to inhibit cellulose production (Evans and

O'Neill 2005). Certain isolates, such as *A. xylinum* sub. sp. *sucrofermentans*, exhibit stability of cellulose synthesis and produce round cellulose balls during agitation, but forming thick pellicles under static growth conditions (Matsuoka et al. 1996). Studies have shown that the bacteria are able to utilize several different carbohydrate sources including glucose, fructose, mannitol, and glycerol, and identified extra-cellular products as well as acidification of the growth media (Herrmann and Neuschul 1931). When grown on glucose as the carbon source, most of the glucose in the growth media is oxidized extracellularly to gluconic acid with concomitant acidification. Ethanol is oxidized to acetic acid, which also results in acidification. A high proportion of glycerol is converted to dihydroxyacetone which can be detected in the growth media (Herrmann and Neuschul 1931). Isotopic labeling experiments have found redistribution of non-exchangeable hydrogens from C6 to C1 and C2 in cellulose produced by *A. xylinum* grown on glucose deuterated at C6 (Gagnaire and Taravel 1975). This result can be explained by the action of the pentose phosphate pathway enzymes hexose phosphate isomerase, phosphofructose kinase, triose phosphate isomerase and aldolase inside the bacterial cell, which would result in redistribution of the isotopic label. Cellulose production using ^{13}C labeled glucose found a similar pattern of redistribution of isotopic labels in the resultant cellulose (Arashida et al. 1993). The isotopic redistribution was found to be reduced and conversion of glucose to cellulose increased by the addition of lactate or ethanol to the media (Arashida et al. 1993). Some strains do not grow well on sucrose, while others grow well on this sugar (Brown 1886; Bernardo et al. 1998). The bacteria oxidize ethanol, acetate, and lactate, and addition of these compounds to growth media containing glucose, fructose, or sucrose has been reported to increase cellulose yields (Krystynowicz et al. 2002; Matsuoka et al. 1996). Development of effective defined minimal media formulations have enabled investigation of nutritional needs and increased cellulose yields (Son et al. 2003; Sano et al. 2010; Matsuoka et al. 1996).

Neutron scattering techniques have recently been used for biomass characterization, in particular to carry out structural analysis and dynamic characterization of its deconstruction (Pingali et al. 2010). The aim of this work is to develop an approach for

controlled incorporation of deuterium into bacterial cellulose. By replacing hydrogen with deuterium in biopolymers such as cellulose it will be possible to obtain a more detailed analysis of the structural and dynamic properties of cellulose using advanced neutron scattering methods (Byron and Gilbert 2000; Melnichenko and Wignall 2007; Nishiyama et al. 1999; Pingali et al. 2010). Previously reported studies used incorporation of deuterium into bacterial cellulose from deuterated glucose and D_2O in growth medium to examine cellulose biosynthetic pathways. Incorporation at non-exchangeable positions in the resultant cellulose was determined by acetylation followed by ^1H NMR (Gagnaire and Taravel 1975; Barnoud et al. 1971). In this work we describe an approach for controlled incorporation of deuterium into bacterial cellulose. The properties of the deuterated cellulose were investigated by Fourier Transform Infra-red spectroscopy (FTIR), mass spectrometry and small-angle neutron scattering (SANS).

Materials and methods

Production of bacterial cellulose

The bacterial strain *A. xylinus* subsp. *sucrofermentans* (ATCC 700178) was purchased from the American Type Culture Collection (Manassas, Virginia, USA). Deuterated glycerol (D_8 , 99 %) was obtained from Cambridge Isotope Laboratory (Andover, Massachusetts, USA).

A. xylinus subsp. *sucrofermentans* (ATCC 700178) was cultivated in a defined growth medium that was formulated based on previously published approaches (Son et al. 2003; Sano et al. 2010; Matsuoka et al. 1996). The growth medium contained 40 g/L glycerol, 4 mL/L 10 % sodium lactate in H_2O , 10 mL/L vitamin stock solution, 10 mL/L mineral salts stock solution, in a basal salt solution which consisted of 2 g/L $(\text{NH}_4)_2\text{SO}_4$, 3 g/L KH_2PO_4 , 3 g/L $\text{Na}_2\text{HPO}_4 \cdot 12\text{H}_2\text{O}$, 0.8 g/L MgSO_4 , and 0.003 g/L boric acid in deionized distilled water. The pH was adjusted to 5.5 with dilute sulfuric acid. Composition of the vitamin stock solution was 200 mg/L inositol, 40 mg/L nicotinic acid, 40 mg/L pyridoxal hydrochloride, 40 mg/L thiamine hydrochloride, 20 mg/L calcium D-pantothenate, 20 mg/L riboflavin,

20 mg/L *p*-amino benzoic acid, 0.2 mg/L D-biotin and 0.2 mg/L folic acid. The mineral salts stock solution contained 360 mg/L $\text{FeSO}_4 \cdot 7\text{H}_2\text{O}$, 1,470 mg/L $\text{CaCl}_2 \cdot \text{H}_2\text{O}$, 242 mg/L $\text{Na}_2\text{MoO}_4 \cdot 2\text{H}_2\text{O}$, 173 mg/L $\text{ZnSO}_4 \cdot 7\text{H}_2\text{O}$, 139 mg/L $\text{MnSO}_4 \cdot 5\text{H}_2\text{O}$, and 5 mg/L $\text{CuSO}_4 \cdot 5\text{H}_2\text{O}$. The mineral salts solution and basal salts solution were sterilized by autoclaving at 121 °C and cooled to room temperature before mixing. The vitamin stock solution and Na-lactate solutions were filter-sterilized with 0.2 µm pore size Nalgene Bottle-Top Sterile Filter Units. The deuterated version of the media was prepared in the same manner except that the salt, lactate, and vitamin solutions were prepared in 99.7 % D_2O and filter sterilized. The cells were adapted to grow in D_2O by sequentially increasing the D_2O concentration in the growth medium with protiated glycerol (*H*-glycerol) as the carbon source, and finally replacing the carbon source with deuterated glycerol (*D*-glycerol) for production of perdeuterated cellulose. For cellulose production, the stock culture of D_2O -adapted cells was sub-cultured into 50 ml of growth medium (1:5 dilution) and grown in 32-oz polypropylene plant culture vessels with lids (Phyto-Technology Laboratories, Shawnee Mission, Kansas, USA) at 25 °C for 14 days under static conditions.

Cellulose purification

The cellulose pellicle was washed with 500 mL deionized H_2O at room temperature followed by 250 mL of water and heating to 90 °C. The pellicle was then soaked in 1 % NaOH at room temperature to remove the bacterial debris. The NaOH solution was replaced several times until the A_{280} absorbance value was <0.01. The cellulose was neutralized by dialysis against 10 L deionized H_2O overnight. The final pH of the liquid surrounding the cellulose was approximately 7–8. The yield of cellulose was typically 0.72 g dry cellulose/L of culture.

FTIR analysis

Bacterial cellulose samples were lyophilized for 3 days. Infrared (FTIR) spectra were measured on a Jasco FT/IR 6100 Series Fourier Transform Infrared Spectrometer in an attenuated total reflectance (ATR) mode. A total of 32 accumulative scans were taken, with a resolution of 1 cm^{-1} , in the range of $4,000\text{--}650 \text{ cm}^{-1}$.

Mass spectrometry analysis

The sample was prepared for mass spectrometry analysis as follows: The cellulose (0.1 % w/v; assuming 100 % glucan content) was hydrolyzed by commercial cellulase cocktail (Accellerase 1500, 0.1 g/g cellulose enzyme loading) in a 7 ml reaction volume (pH 4.8, 50 mM citrate buffer in water) for 24 h at 50 °C, and 250 rpm (Gao et al. 2010). After completion of hydrolysis, HPLC-refractive index (RI) analysis was then carried out to estimate total protiated (*H*-glucose) or deuterated glucose (*D*-glucose) concentration in the bacterial cellulose hydrolysate as described previously (Chundawat et al. 2010). Identical retention times and RI integrated peak areas (to within 5 %) were observed for both labeled and unlabeled sugar standards during the HPLC-RI analysis. The hydrolysate was further cleaned up to remove background proteins that interfere with LC-MS analysis, as described elsewhere (McIntosh et al. 2002). LC-MS analysis was carried out using a QTRAP 3200 mass spectrometer (AB/Sciex) coupled to a binary LC-20AD pump, CTO-10Avp column oven, and Sil-HTc autosampler (Shimadzu). Separations were conducted by injection of a 5.0 µL aliquot onto a Prevail Carbohydrate ES column (Grace) that was held at 40 °C. Total mobile phase flow rates was 0.25 mL/min, using Solvent A (10 mM aqueous ammonium acetate) and Solvent B (acetonitrile) using the following gradient (A/B): initial (25/75), linear gradient to 5.0 min (50/50) followed by a hold until 6.0 min; at 6.01 min the composition was returned to the initial condition and held there until 8 min. Mass spectrometry analyses employed electrospray ionization in negative ion mode, using an ion source temperature of 450 °C. Both Gas1 and Gas2 flows were set to 45 (arbitrary units). Quantification of abundances of individual ions from m/z 179.1 to 187.1 was performed using Q1 multiple ion monitoring data acquisition with a 25 ms dwell time for each nominal mass. Confirmatory analyses were also performed in positive ion mode. Individual ion abundances were determined by manually integrating each extracted ion chromatogram using Analyst software (Ver 1.4.2, AB/SCIEX, Framingham, MA) and integrated peak areas were exported to text files for analysis. Calibration curve for *H*-glucose and *D*-glucose characteristic ions (m/z 179 and 186, respectively) were linear up to 1 mM (adjusted- R^2

of 0.98) but had a poorer linear-fit at tenfold higher concentrations (adjusted- R^2 of 0.88). The fully deuterated D_{12} -glucose is expected to rapidly exchange deuteriums attached to oxygen with protons from water to give D_7H_5 -glucose. Therefore, for fully-labeled bacterial cellulose we should expect to see D_7H_5 -glucose after enzymatic hydrolysis in water. Enzyme blanks were included (no cellulose present) in the analysis to account for possible interference from unknown molecular species (with similar m/z between 179 and 186) present in the commercial enzyme cocktails.

Small-angle neutron scattering

SANS measurements were performed with the CG-3 Bio-SANS instrument (Lynn et al. 2006) at the High Flux Isotope Reactor (HFIR) facility of Oak Ridge National Laboratory. Cylindrical Hellma cells with 1 mm path length (Model# 120-QS 1.0 mm) were used to perform SANS studies. The three different instrument configurations employed to cover the range, $0.003 < Q \text{ (}\text{\AA}^{-1}\text{)} < 0.4$, of scattering vectors with sufficient overlap were sample-to-detector distances of 2,529, 6,829 and 15,329 mm at 6 Å neutron wavelength. The scattering vector Q ($Q = 4\pi \sin\theta/\lambda$) describes the relation of Q to λ , neutron wavelength and 2θ , the scattering angle. The center of the area detector (1 m × 1 m GE-Reuter Stokes Tube Detector) was offset by 350 mm from the beam. The instrument resolution was defined using circular aperture diameters of 40 mm and 14 mm for source and sample, respectively and separated by distances: 3,262, 9,332 and 17,430 mm. The relative wavelength spread $\Delta\lambda/\lambda$ was set to 0.15. The scattering intensity profiles $I(Q)$ versus Q , were obtained by azimuthally averaging the processed 2D images, which were normalized to incident beam monitor counts, and corrected for detector dark current, pixel sensitivity and scattering from the quartz cell. For the SANS experiments, the cellulose was ground into slurry using a commercial blender for 2 min. The cellulose slurry was centrifuged followed by resuspension in 0, 25, 50, 75, and 100 % D_2O at a 1:10 ratio to exchange the labile hydroxyl hydrogens in the cellulose. This process was repeated three times. The final concentration of cellulose was 0.5 % (w/v).

Results and discussion

Cellulose synthesis

The overall aim of the work was to develop an approach for controlled incorporation of deuterium in bacterial cellulose. The absence of undefined components such as yeast extract or corn steep liquor in the growth medium is important for controlled and reproducible incorporation of deuterium into cellulose. The suitable deuterated carbon sources for bacterial cellulose production that are available commercially are limited to glucose and glycerol. Previously, cellulose production with *A. xylinum* bacteria using a synthetic salts formulation (Son et al. 2003) supplemented with corn steep liquor and fructose as the carbon source was reported (Sano et al. 2010). An earlier study of the growth and cellulose production of *A. xylinus* subsp. *sacrofermentans* had investigated the stimulatory effects of corn steep liquor and determined that lactate was the ingredient that conferred the faster growth (Matsuoka et al. 1996). The authors described mineral and vitamin supplements for preparation of a synthetic defined medium (Matsuoka et al. 1996; Watanabe et al. 1999). Cellulose production tests were carried out to determine the minimal medium additives required to obtain good cellulose formation using *A. xylinus sacrofermentans* (ATCC 700178). The cellulose was purified and quantified, as described in Materials & Methods. Based on these tests, a formulation that did not require the addition of undefined components was devised and shown to produce fast growth and cellulose formation (See Materials & Methods). This formulation, termed Son-Matsuoka-Fructose (SMF), is derived from a combination of those described by Matsuoka et al. and by Son et al. and contains 4 % fructose and 0.04 % sodium DL-lactate with vitamins and minerals. For growth in D_2O media, glycerol, which is commercially available in deuterated form, was substituted for fructose as the carbon source.

FTIR analysis

The protiated and deuterated cellulose samples were equilibrated in H_2O and D_2O , respectively before drying by lyophilization. A comparison of the FTIR spectra of deuterated cellulose and protiated cellulose

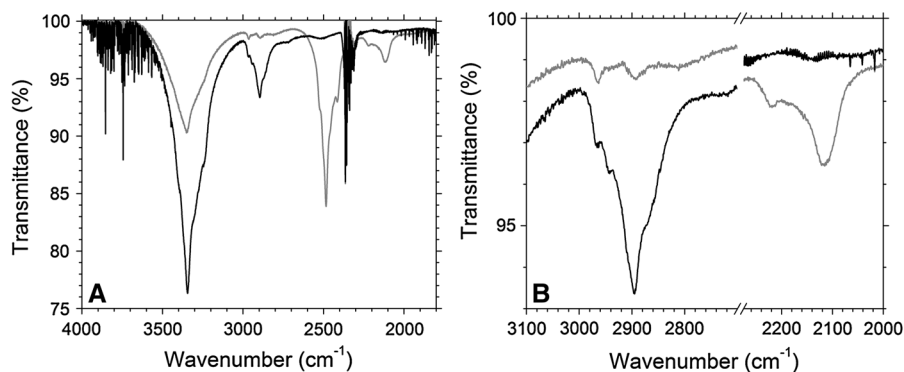


Fig. 1 **a** FTIR-ATR spectra of lyophilized protiated (*black*) and deuterated (*grey*) bacterial cellulose. **b** CH and CD stretching regions of the FTIR spectra

between 4,000 and 1,800 cm^{-1} are shown in Fig. 1. The intensities of the sharp OH-stretching infrared bands located at approximately 3,500 and 3,300 cm^{-1} (Hofstetter et al. 2006) were decreased in the deuterated cellulose sample. This was accompanied by the appearance of an OD stretching band near 2,400 cm^{-1} . The presence of OH stretching in deuterated cellulose is attributed to the presence of hydration water at the surface of the cellulose. The majority of the bands corresponding to the CH stretching modes are located around 3,000–2,800 cm^{-1} (Tashiro and Kobayashi 1991). These bands were largely absent in the deuterated cellulose sample. However, a band appeared at 2,100 cm^{-1} which is assigned to the CD stretching region. This provides strong evidence that the level of deuterium incorporation in the cellulose was very high. Minor differences in the shapes of the CH and CD stretching regions in their respective spectra may be due the presence of a small amount of aliphatic hydrogen in the deuterated cellulose sample that can be observed in its spectrum at $\sim 2,900 \text{ cm}^{-1}$ (Fig. 1b). The anomalous incorporation of hydrogen in the deuterated cellulose could result in glucose residues with CH and CDH groups giving rise to changes in the region associated with CD/CD₂ vibrational stretching. As will be discussed further on the presence of a small amount of aliphatic hydrogen in the deuterated cellulose is confirmed by mass spectrometry analysis.

Mass spectrometry

As described in the “Materials and methods” section the protiated and deuterated cellulose samples were digested with a cellulolytic enzyme cocktail to

hydrolyze cellulose to glucose for rapid analysis by LC–MS. Enzymatic digestion of the protiated cellulose and deuterated cellulose produced $\sim 95 \pm 2$ and $\sim 90 \pm 1$ % of the expected glucose yield, respectively. No other sugars from either cellulose were detected by HPLC-RI in significant concentrations. This gives confidence that the glucose released for subsequent LC–MS is representative of the total labeled and unlabeled carbohydrate content of the cellulose samples analyzed. The marginally higher hydrolysis yields for protiated cellulose versus deuterated cellulose are attributed to secondary kinetic isotope effects (KIE) of the cellulolytic enzyme-catalyzed deconstruction of cellulose to cellobiose and finally glucose. However, a more detailed investigation using purified cellulases will be necessary to verify this considering that glycosidase mechanisms are difficult to discern from secondary KIE’s (Vasella et al. 2002). The LC–MS analysis was performed using total glucose concentrations ranging from 1 to 10 mM.

A summary of the LC–MS analytical results is shown in Fig. 2. The pseudomolecular ion peaks at m/z 179 for $[\text{M}-\text{H}]^-$ of unlabeled glucose and m/z 186 of D_7 -glucose are evident. Surprisingly, the relative abundance ratios A_{185}/A_{186} and A_{184}/A_{186} , which reflect percent molar ratios of D_6 to D_7 -glucose and D_5 to D_7 -glucose, differ between the deuterated cellulose hydrolysate and the D -glucose standard (Table 1), and are consistent with incomplete deuteration. The anomalous incorporation of varying amounts of D atoms into cellulose could be due to either slow condensation of H₂O moisture within the culture tube that exchanged slowly with

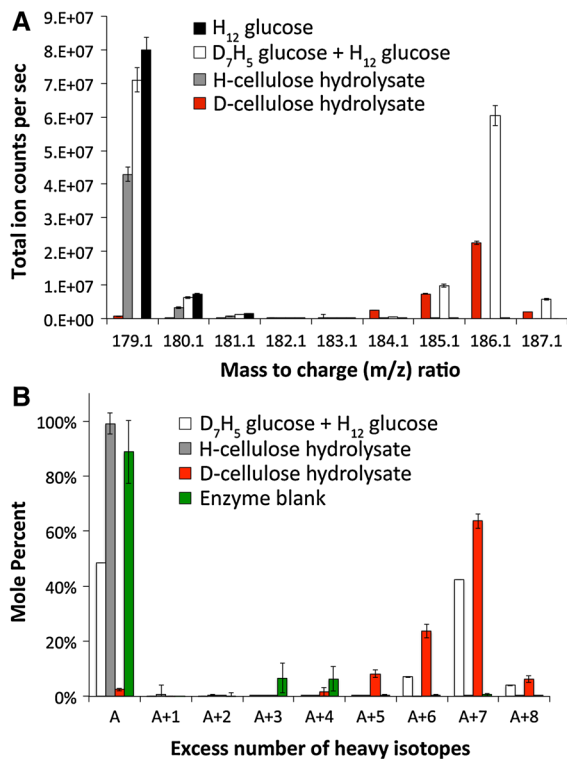


Fig. 2 **a** Relative ion abundance and **b** calculated mole percent of major molecular species in hydrolysis products of deuterated and unlabeled cellulose. LC–MS was carried out under Q1 multiple ion monitoring using electrospray ionization in negative-ion mode to detect pseudomolecular ion ($[M-H]^-$) species in the range of m/z 179–187. Note that D_7H_5 -glucose + H_{12} -glucose is an equimolar mixture of each. Error bars represent standard deviations for duplicate hydrolysate reaction mixtures. Mole percent of heavy isotopes relative to the unlabeled species (m/z 179) was calculated based on the procedure described by Biemann (1962)

Table 1 Molar abundance (A) ratios of different mass to charge (m/z) species detected in the negative-ion mode LC–MS analyses of hydrolysates of *protiated* and *deuterated* cellulose

Sample description	A_{185}/A_{186}	A_{184}/A_{186}
D_7H_5 -glucose + H_{12} -glucose	0.17	0.01
H-cellulose hydrolysate	ND	ND
D-cellulose hydrolysate	0.37	0.13

Ratios were only estimated for peaks with total ion counts greater than 10^5 counts per second as shown in Fig. 2. ND stands for not detected. Reported ratios are means from duplicate hydrolysate reaction mixtures

the heavy water and caused protonation of intermediates involved in cellulose synthesis. Or, more interestingly, the conversion of the unlabeled lactate

into pyruvate, which is finally taken up for cellulose biogenesis could also explain the anomalous levels of D atoms incorporation into cellulose. Previous work has shown lactate can stimulate bacterial cellulose production by stimulating cell growth by generating energy for growth (Matsuoka et al. 1996). More importantly, it has been shown that *A.* produces a unique pyruvate-phosphate dikinase that catalyzes the direct phosphorylation of pyruvate into phosphoenol-pyruvate that can be directly assimilated into the production of cellulose (Benziman and Eizen 1971). Nevertheless, our analysis suggests a high level of deuterium incorporation into deuterated cellulose samples. The total *D*-glucose incorporated into the bacterial cellulose (calculated using the peaks likely representative of $[M-H]^-$ based D_7 , D_6 , and D_5 glucose and the integrated peak areas from m/z 184–186) indicates that 97 % of glucose subunits contain at least five deuterium atoms.

SANS analysis

SANS was used to compare the nano-scale structural features of bacterial cellulose with different levels of deuterium incorporation. Figure 3a shows the scattering profiles recorded at a cellulose concentration of 0.5 % w/v in 100 % H_2O (maximum contrast between the cellulose and the solvent) for cellulose grown in different *D*-Glycerol/*H*-Glycerol ratios 100, 50, 40, 30, and 0 %. The curves look similar without significant differences in structural features. A contrast variation series was performed by varying the H_2O/D_2O ratio of the solvent between 0 and 100 % D_2O . At a Q value that shows enhanced contrast variation, the relation of scattering intensity versus ratio of D_2O in solvent was fit to a parabola and scattering length density (SLD) associated with the ratio of D_2O at the vertex is the contrast match SLD. The relation between SLD, obtained by performing contrast variation study for each cellulose variant, and *D*-Glycerol ratio used to produce those samples is shown in Fig. 3b. The relation demonstrates that by varying the amount of deuterated carbon source added to the growth medium it is possible to control the level of deuterium incorporation into the cellulose molecules.

All scattering curves monotonically increase in scattering intensity for smaller wave-vectors, Q , exhibiting a power-law dependence with an exponent of -2 (Fig. 4a). An exponent of -2 implies that

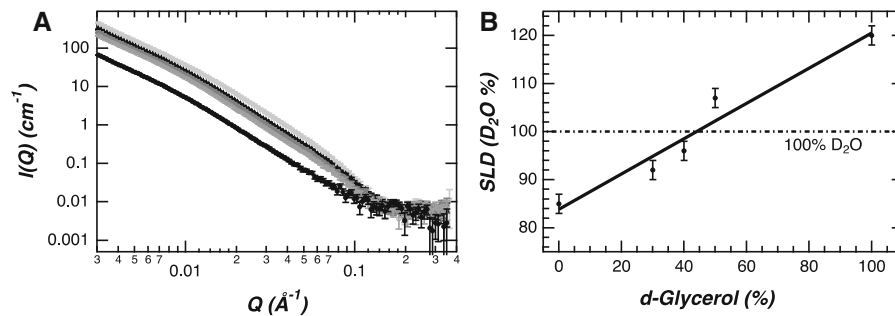


Fig. 3 SANS analysis of purified bacterial cellulose with different levels of deuterium incorporation. (A) SANS profiles of celluloses grown using 100, 50, 40, 30 and 0 % *D*-glycerol (light grey dots to black dots) measured in 100 % H_2O .

b Scattering length densities (SLD) of different cellulose samples related to the fraction of *D*-glycerol present in the growth medium

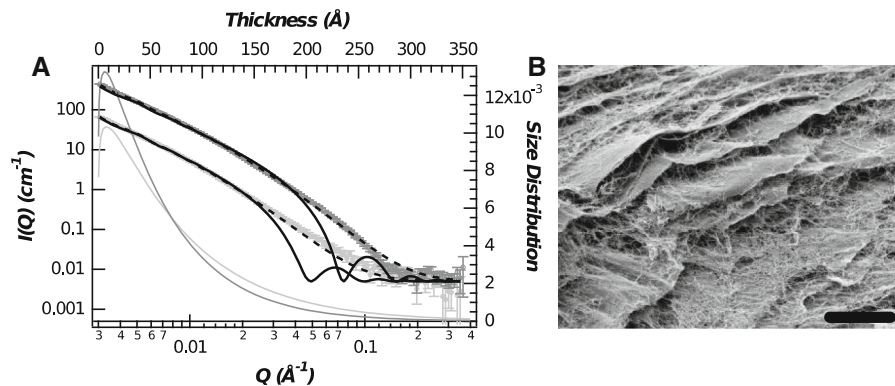


Fig. 4 SANS analysis of purified bacterial cellulose with 0 and 100 % deuterium incorporation. **a** SANS profiles of celluloses grown using 100 % (dark grey open circles) and 0 % (light grey dots) *D*-Glycerol measured in 100 % H_2O . Large disks (closest approximation to sheet-like forms) with monodisperse thickness (solid black lines) and Schulz's polydisperse thickness (dashed

black lines) were used as models to fit data. The thickness distribution (100 and 0 % *D*-Glycerol—dark and light grey lines respectively) is plotted against the thickness (top) versus size distribution (right). **b** SEM image of protiated bacterial cellulose (scale bar 50 μm)

deuterated bacterial cellulose represents disk like forms as seen by SEM (Fig. 4b). A large disk model was used to fit the curves of bacterial cellulose grown using 0 and 100 % *D*-Glycerol. The most important aspect of our fits, large disk with monodisperse or polydisperse thickness is that the thickness of the disk are comparable between the bacterial cellulose grown using 0 and 100 % *D*-Glycerol suggesting minimal structural effect on deuterium incorporation into bacterial cellulose. The fits using the monodisperse function provide a lower bound to the disk radius, $R_{\min} = 1,132 \pm 6$ and $1,154 \pm 3 \text{ \AA}$ and the disk thickness, $T = 128 \pm 1$ and $83 \pm 1 \text{ \AA}$ for the protiated and deuterated forms of the bacterial cellulose,

respectively. Schulz's polydispersity in disk thickness also provides a lower bound for disk radius, $R = 1,158 \pm 6$ and $1,158 \pm 3 \text{ \AA}$ and average disk thickness, $T_{\text{avg}} = 80 \pm 2$ and $62 \pm 1 \text{ \AA}$ for protiated and deuterated bacterial cellulose, respectively. The polydispersity index for both curves tend to the highest level of polydispersity (0.95 was the upper bound on that parameter). The SEM image in Fig. 4b shows features that can be related to cellulose sheets and fibers. All these features will have comparable contributions in the high- Q region ($Q > 0.05 \text{ \AA}^{-1}$) which explains the reason for some discrepancy in agreement between experimental data and the fits that purely model large disk structures.

Conclusions

This study shows that deuterium incorporation into bacterial cellulose can be varied by altering the ratio of deuterated and protiated glycerol used during cell growth in a D₂O-based growth medium. Spectrophotometric analysis and mass spectrometry show that the level of deuterium incorporation is high (>90 %) for the perdeuterated form of bacterial cellulose. This is consistent with the results from a previous investigation using nuclear magnetic resonance to characterize deuterated bacterial cellulose (Bali et al. 2013). The SANS profiles of the cellulose are all similar indicating that there are no structural changes in the cellulose due to substitution of deuterium for hydrogen. Previous powder x-ray diffraction and scanning electron microscopy of deuterated cellulose also support this observation (Bali et al. 2013). This material will have a wide range of applications in elastic and inelastic neutron scattering experiments for studying aspects of cellulose structure and dynamics. The large difference in the scattering cross-sections of hydrogen and deuterium introduces contrast between different components in a system which would not be possible with natural abundance isotopic forms of the same material. Using this approach it is possible to carry out structural studies such as investigating the interaction of enzymes with cellulose and also dynamic studies such as investigating water diffusion on the surface of cellulose.

Acknowledgments This research is funded by the Genomic Science Program, Office of Biological and Environmental Research, U.S. Department of Energy, under FWP ERKP752. The Center for Structural Molecular Biology (Project ERKP291) and the Bio-SANS beam line is supported by the Office of Biological and Environmental Research U.S. Department of Energy. Research at the Spallation Neutron Source and High Flux Isotope Reactor at Oak Ridge National Laboratory (ORNL) are supported by the Scientific User Facilities Division, Office of Basic Energy Sciences, U.S. Department of Energy (DOE). ORNL is managed by UT Battelle, LLC, for the U.S. DOE under Contract No. DE-AC05-00OR22725. SPSC acknowledges support from the DOE Great Lakes Bioenergy Research Center (DE-FC02-07ER64494) and Prof. Bruce Dale from Michigan State University. We appreciate support from the Michigan State University Mass Spectrometry and Metabolomics Core for LC-MS method development and execution. ADJ acknowledges support from Michigan AgBioResearch.

References

- Arashida T, Ishino T, Kai A (1993) Biosynthesis of cellulose from culture media containing ¹³C-labeled glucose as a carbon source. *J Carbohydr Chem* 12:641–649
- Bali G, Foston MB, O'Neill HM, Evans BR, He J, Ragauskas AJ (2013) The effect of deuteration on the structure of bacterial cellulose. *Carbohydr Res* 374:82–88
- Barnoud F, Gagnaire D, Odier L, Vincendon M (1971) Biosynthèse de la cellulose bactérienne deutérée: étude par R. M. N. du taux d'incorporation et de la localisation du deutérium. *Biopolymers* 10:2269–2273
- Benziman M, Eizen N (1971) Pyruvate-phosphate dikinase and the control of gluconeogenesis in *Acetobacter xylinum*. *J Biol Chem* 246:57–61
- Bernardo EB, Neilan BA, Couperwaite I (1998) In vitro characterization, differentiation, and identification of wild-type cellulose-synthesizing acetobacter strains involved in Nata de Coco production. *Syst Appl Microbiol* 21:599–608
- Biemann K (1962) Mass spectrometry: organic chemical applications. McGraw-Hill, NY
- Brown A (1886) On an acetic ferment which forms cellulose. *J Chem Soc* 49:432–439
- Byron O, Gilbert RJ (2000) Neutron scattering: good news for biotechnology. *Curr Opin Biotechnol* 11:72–80
- Cannon RE, Anderson SM (1991) SM biogenesis of bacterial cellulose. *Crit Rev Microbiol* 17(6):435–447
- Chundawat SPS, Vismeh R, Sharma LN, Humpala JF, da Costa Sousa L, Chambliss CK, Jones AD, Balan V, Dale BE (2010) Multifaceted characterization of cell wall decomposition products formed during ammonia fiber expansion (AFEX) and dilute-acid based pretreatments. *Biores Technol* 101:8429–8438
- Czaja WK, Young DJ, Kawecki M, Brown RM Jr (2007) The future prospects of microbial cellulose in biomedical applications. *Biomacromolecules* 8(1):1–12
- Evans BR, O'Neill HM (2005) Effect of surface attachment on synthesis of bacterial cellulose. *Appl Biochem Biotechnol* 121:439–450
- Evans BR, O'Neill HM, Malyvanh VP, Lee I, Woodward J (2003) Palladium-bacterial cellulose membranes for fuel cells. *Biosens Bioelectron* 18(7):917–923
- Franz G, Blaschek W (1990) Chapter 8, "Cellulose". In: Day PM, Harborne JB (eds) *Methods in plant biochemistry*, vol 2. Academic Press, London, pp 291–322
- Gagnaire D, Taravel FR (1975) Biosynthesis of bacterial cellulose from glucose selectively deuterated in position 6: NMR study. *FEBS Lett* 60:317–321
- Gao D, Chundawat SPS, Krishnan C, Balan V, Dale BE (2010) Mixture optimization of six core glycosyl hydrolases for maximizing saccharification of ammonia fiber expansion (AFEX) pretreated corn stover. *Biores Technol* 101(8):2770–2781
- Herrmann S, Neuschul P (1931) Zur Biochemie der Essigbakterien, zugleich ein Vorschlag fuer eine neue Systematik. *Biochemische Zeitschrift* 233:129–216
- Hestrin S, Schramm M (1954) Synthesis of cellulose by *Acetobacter xylinum*. 2. Preparation of freeze-dried cells capable of polymerizing glucose to cellulose. *Biochem J* 58:345–352

- Himmel ME, Ding SY, Johnson DK, Adney WS, Nimlos MR, Brady JW, Foust TD (2007) Biomass recalcitrance: engineering plants and enzymes for biofuels production. *Science* 315:804–807
- Hofstetter K, Hinterstoisser B, Salmén L (2006) Moisture uptake in native cellulose: the roles of different hydrogen bonds: a dynamic FT-IR study using Deuterium exchange. *Cellulose* 13:131–145
- Holt JG, Krieg NR, Sneath PHA, Staley JH, Williams ST (1994) *Wilkinson Bergey's manual of determinative bacteriology*, 9th ed
- Iguchi M, Yamanaka S, Budhiono A (2000) Bacterial cellulose—a masterpiece of nature's arts. *J Mater Sci* 35:261–270
- Kawano S, Tajima K, Uemori Y, Yamashita H, Erata T, Munekata M, Takai M (2002) Cloning of cellulose synthesis related genes from *Acetobacter xylinum* ATCC 23769 and ATCC 53582. *DNA Res* 9:149–156
- Klemm D, Heublein B, Fink H-P, Bohn A (2005) Cellulose: fascinating biopolymer and sustainable raw material. *Angew Chem* 44:2–37
- Krystynowicz A, Czaja W, Wiktoroskowa-Jeziarska A, Goncalvez-Miškiewicz M, Turkiewicz M, Bielecki SJ (2002) Factors affecting yield and properties of bacterial cellulose. *J Indust Microbiol Biotechnol* 29:189–195
- Lynn GW, Heller W, Urban V, Wignall GD, Weiss K, Myles DA (2006) Bio-SANS-A dedicated facility for neutron structural biology at Oak Ridge National Laboratory. *Physica B* 385–386:880–882
- Matsuoka M, Tsuchida T, Matsushita K, Adachi O, Yoshinaga F (1996) A synthetic medium for bacterial cellulose production by *Acetobacter xylinum* subsp. *Sacrofermentans*. *Biosci Biotech Biochem* 68:575–579
- McIntosh TS, Davis HM, Matthews DE (2002) A liquid chromatography-mass spectrometry method to measure stable isotopic tracer enrichments of glycerol and glucose in human serum. *Anal Biochem* 300(2):163–169
- Melnichenko YB, Wignall GDJ (2007) Small-angle neutron scattering in materials science: recent practical applications. *Appl Phys* 102:021101
- Nishiyama Y, Okano T, Langan P, Chanzy H (1999) Cellulose structure studied by high resolution fibre neutron diffraction. *Int J Biol Macromol* 26:279–283
- Pérez S et al (2010) Structure and engineering of celluloses. *Advances in carbohydrate chemistry and biochemistry*. Academic Press 64:25–116
- Pingali SV, Urban VS, Heller WT, McGaughey J, O'Neill HM, Foston M, Myles DA, Ragauskas AJ, Evans BR (2010) SANS study of cellulose extracted from switchgrass. *Acta Crystallogr Sect D* 66:1189–1193
- Ragauskas AJ, Williams CK, Davison BH, Britovsek G, Cairney J, Eckert CA, Frederick WJ Jr, Hallett Jp, Leak DJ, Liotta CL, Mielenz JR, Murphy R, Templer R, Tschaplinski T (2006) The path forward for biofuels and biomaterials. *Science* 311:484–489
- Sano MB, Rojas AD, Gatenholm P, Davalos RV (2010) Dielectrophoretic Microweaving: biofabrication of aligned bacterial cellulose nanofibrils. *Ann Biomed Engr* 38:2475–2484
- Saxena IM, Kudlicka K, Okuda K, Brown RM Jr (1994) Characterization of genes in the cellulose-synthesizing operon (acs operon) of *Acetobacter xylinum*: implications for cellulose crystallization. *J Bacteriol* 176(18):5735–5752
- Schramm M, Hestrin S (1954) Factors affecting production of cellulose at the air-liquid interface of a culture of *Acetobacter xylinum*. *J Gen Microbiol* 11:123–129
- Shah J, Brown RM Jr (2005) Towards electronic paper displays made from microbial cellulose. *Appl Microbiol Biotechnol* 66:352–355
- Son HJ, Kim HG, Kim KK, Kim YG, Lee SJ (2003) Increased production of bacterial cellulose by *Acetobacter* sp. V6 in synthetic media under shaking culture conditions. *Biores Technol*. 86:215–219
- Tashiro K, Kobayashi M (1991) Theoretical evaluation of three-dimensional elastic constants of native and regenerated cellulose: role of hydrogen bonds. *Polymer* 32(8):1516–1526
- Vasella A, Davies GJ, Bohm M (2002) Glycosidase mechanisms. *Curr Opin Chem Biol* 6(5):619–629
- Yamada Y, Hoshino K, Ishikawa T (1997) The phylogeny of acetic acid bacteria based on the partial sequences of 16S ribosomal RNA: the elevation of the subgenus *Gluconoacetobacter* to the generic level. *Biosci Biotechnol Biochem* 61(8):1244–1251
- Watanabe K, Takemura H, Tabuchi H, Tabuchi M, Tahara N, Toyosaki H, Marinaga Y, Tsuchida T, Yano H, Yoshinaga F (1999) Cellulose-producing bacteria. US Patent 5,962,277